

Original Paper

# Evaluation of Stem Cell Laden Collagen + Polycaprolactone + Multi-Walled Carbon Nano-Tubes Nano-Neural Scaffold with and Without Insulin Like Growth Factor-I For Sciatic Nerve Regeneration Post Crush Injury in Wistar Rats

Mamta Mishra<sup>a</sup> Swapan Kumar Maiti<sup>a</sup> Kalaiselvan Elangovan<sup>a</sup>  
Shivaraju Shivaramu<sup>a</sup> Karam Pal Singh<sup>b</sup> Amitha Banu S<sup>a</sup> Merlin Mamachan<sup>a</sup>  
Manish Arya<sup>a</sup> Divya Mishra<sup>c</sup> Jurgen Hescheler<sup>d</sup>

<sup>a</sup>Division of Veterinary Surgery and Radiology, ICAR-Indian Veterinary Research Institute, Izatnagar, Bareilly, Uttar Pradesh, India, <sup>b</sup>CADRAD, ICAR-Indian Veterinary Research Institute, Izatnagar, Bareilly, Uttar Pradesh, India, <sup>c</sup>Division of Animal Biotechnology, ICAR-Indian Veterinary Research Institute, Izatnagar, Bareilly, Uttar Pradesh, India, <sup>d</sup>Institute of Neurophysiology, University of Cologne, Cologne, Germany

## Key Words

Sciatic Crush Injury • Nerve regeneration • Carbon nanotubes • Stem cell • Insulin-like Growth Factor I (IGF-I) • Histopathology • Scanning Electron Microscopy

## Abstract

**Background/Aims:** All body functions are activated, synchronized and controlled by a substantial, complex network, the nervous system. Upon injury, pathophysiology of the nerve injury proceeds through different paths. The axon may undergo a degenerative retraction from the site of injury for a short distance unless the injury is near to the cell body, in which case it continues to the soma and undergoes retrograde neuronal degeneration. Otherwise, the distal section suffers from Wallerian degeneration, which is marked by axonal swelling, spheroids, and cytoskeleton degeneration. The objective of the study was to evaluate the potential of mesenchymal stem cell laden neural scaffold and insulin-like growth factor I (IGF-I) in nerve regeneration following sciatic nerve injury in a rat model. **Methods:** The animals were anaesthetized and a cranio-lateral incision over left thigh was made. Sciatic nerve was exposed and crush injury was introduced for 90 seconds using haemostat at second locking position. The muscle and skin were sutured in routine fashion and thus the rat model of sciatic

crush injury was prepared. The animal models were equally distributed into 5 different groups namely A, B, C, D and E and treated with phosphate buffer saline (PBS), carbon nanotubes based neural scaffold only, scaffold with IGF-I, stem cell laden scaffold and stem cell laden scaffold with IGF-I respectively. *In vitro* scaffold testing was performed. The nerve regeneration was assessed based on physico-neuronal, biochemical, histopathological examination, and relative expression of NRP-1, NRP-2 and GAP-43 and scanning electron microscopy. **Results:** Sciatic nerve injury model with crush injury produced for 90 seconds was standardized and successfully used in this study. All the biochemical parameters were in normal range in all the groups indicating no scaffold related changes. Physico-neuronal, histopathological, relative gene expression and scanning electron microscopy observations revealed appreciable nerve regeneration in groups E and D, followed by C and B. Restricted to no regeneration was observed in group A. **Conclusion:** Carbon nanotubes based scaffold provided electro-conductivity for proper neuronal regeneration while rat bone marrow-derived mesenchymal stem cells were found to induce axonal sprouting, cellular transformation; whereas IGF-I induced stem cell differentiation, myelin synthesis, angiogenesis and muscle differentiation.

© 2023 The Author(s). Published by  
Cell Physiol Biochem Press GmbH&Co. KG

## Introduction

Peripheral Nerve injury (PNI) is one of the paramount pathology encountered in animals leading to partial or total loss of motor, sensory and autonomic functions transmitted by the injured nerves to the denervated segments of the body, due to interference with the axonal continuity, neuronal degeneration distal to the site of injury and ultimate apoptosis of axotomized neurons [1]. Prompting causes of peripheral nerve injury includes penetrating injury, crush, ischemia, traction, electric and thermal shock, radiation, vibration and percussion causing broad spectrum of clinical symptoms, ranging from slight paraesthesia and pain to weakness or paralysis of muscle [2]. Peripheral nerve injury is also a frequent collateral effect of surgical interventions [3], e.g., in pelvic surgery, the damage to visceral nerves frequently causes bladder, bowel, and/or sexual dysfunction.

Mesenchymal stem cells have a high degree of flexibility, which makes them useful in tissue engineering. Their exceptional immune-modulatory characteristic, as well as their capacity to attract themselves to the site of injury, makes them a „natural *in vivo* system for tissue healing”. Polycaprolactone scaffolds have a higher mechanical strength than natural polymers, are highly biocompatible, have a flexible shape, and can be processed in a controlled manner, allowing for optimal anatomical fit. As it has been proven in comparable biomaterials, Multi-walled carbon nanotubes (MWCNTs) are emerging as a promising therapy option for neurological diseases and injured nerve tissue. MWCNTs have morphological similarities to neurites, and short carbon nanotubes (CNT) bundles have dimensions comparable to dendrites (branched extensions of neuron cells), expanding possibilities for investigating, mending, activating, or reconfiguring brain networks, as well as gaining insights into basic neuronal operations [4]. CNT + Collagen polymer improves electrical conductivity, resulting in good survival of neuronal cells. By modulating the inflammatory and early proliferative stages of nerve repair, local augmentation of insulin-like growth factor I at the crush injury site may promote axonal sprouting. IGF-I administration to the crush-injured location may hasten the functionalization of paralysed muscle by enhancing the pace of recovery. Therefore, the study was intended to investigate the potential of carbon nanotubes based scaffold, mesenchymal stem cells and IGF-I in promoting nerve regeneration following crush injury in rat model.

## Materials and Methods

### Preparation of Scaffold

The composite Nano-neural scaffold with the dimension of 20 mm x 5 mm x 0.05 mm was made of collagen + polycaprolactone (PCL) + multi-walled carbon nanotubes (MWCNT) in 7.5:2.5 percentage by weight (wt %) blend of collagen (collagen from natural source) and polycaprolactone along with 0.5 wt % concentration of randomly arranged carbon nanotubes. Cross linking strategies of pure collagen scaffold enhance the mechanical and structural properties, but may introduce negative effects too on cellular response *in vivo*. Thus, in this study a mixture of natural and synthetic polymer (PCL) reinforced with MWCNT has been used. It was prepared using electro-spinning process at Indian Institute of Technology (IIT) at Roorkee. The scaffolds were supplied to IVRI for this research work.

### *In vitro* testing of the scaffold

Result of scanning electron microscopic surface morphology revealed the scaffold being constructed without the use of an electric field, therefore the cross-sectional surface of the scaffolds containing MWCNTs had a rough surface and a dispersed distribution of MWCNTs.

Utilizing uniaxial tensile testing, the mechanical behaviour of the scaffolds was investigated. Tensile tests were performed on scaffold which evident that adding reinforcement made of MWCNT significantly increases the scaffolds' ability to support loads. The Young's Modulus (E) of the scaffolds reinforced with random MWCNTs, i.e. Collagen + PCL + MWCNT were found to be  $141 \pm 3.8$ .

In MWCNT based scaffolds, the electrical conductivity in the direction of alignment was  $0.000035 (\pm 0.0000049)$  S/m. Overall, these findings show that the scaffolds can be given greater conductivity, which stimulates the differentiation of neurons, by strengthening the MWCNTs within the polymeric matrix.

The surface roughness may be a contributing factor in the deterioration of the scaffolds. In comparison to scaffolds with less rough surfaces, those with enhanced surface roughness may have more exposed polymeric chain ends for the enzymes to act on, leading to increased breakdown. Surface roughness was reported to be 83% higher for MWCNT scaffolds.

Another crucial element for the appropriateness of the scaffold is the biodegradation of the tissue-engineered scaffolds. MWCNT containing scaffolds deteriorated more quickly. Briefly, the degradation of Collagen + PCL + MWCNT scaffold was found to be  $41.1 \pm 2.2\%$  after 60 days.

### Experimental designs

The study was designed after getting permission from Institutional Animal Ethical Committee (IAEC) against No. IAEC/10.03.2023/S32. Healthy adult male Wistar rats weighing around 200 – 300 g between 2-3 months of age were used throughout the study. Animals were procured from the laboratory Animal Resources (LAR) section of the institute. Rats were maintained in polyethylene cages with food and water *ad libitum* in a laboratory with controlled ambient temperature. The experimental animal models of sciatic nerve crush injury were prepared in seventy-five animals and randomly divided into 5 groups, namely, Groups A, B, C, D and E having 15 animals in each group. Animals of each group were given treatment according to Table 1.

The animals were sacrificed on 30<sup>th</sup>, 60<sup>th</sup> and 90<sup>th</sup> day and gastrocnemius muscle and sciatic nerve samples were collected for histopathology, scanning electron microscopy and relative gene expression studies. The blood samples were also collected at similar time intervals; serum was separated from it and subjected to biochemical analysis.

**Table 1.** Treatment protocol for animals in different groups

Sr No.	Group	Number of animals (rat)	Treatment
1	A	15	Phosphate buffered saline (control)
2	B	15	Implanted with randomly aligned Collagen + PCL +MWCNT at the site of injury
3	C	15	Implanted with randomly aligned Collagen + PCL + MWCNT and instilled with IGF-I on 0, 3,7,14, 21 and 28 days at the site of injury
4	D	15	implanted with stem cell laden randomly aligned Collagen + PCL + MWCNT at the site of injury
5	E	15	Implanted with stem cell laden randomly aligned Collagen + PCL + MWCNT and instilled with IGF-I on 0, 3,7,14, 21 and 28 days at the site of injury

### Isolation, collection and cultivation of mesenchymal stem cells from rat

Bone marrow was collected from femur and tibia of adult Wistar rat. Aseptic preparation was made at the collection site after euthanizing the animal. The epiphysis and metaphysis of the long bones were cut with a manual bone saw after the femur and tibia were gathered and meticulously cleaned. After that, by flushing complete culture media (Dulbecco's modified eagles medium-low Glucose (DMEM-LG), 15% fetal bovine serum, 1% penicillin-G and streptomycin) via the diaphyseal canal bone marrow was obtained into a falcon tube with a 15 ml capacity. Following the collection of marrow aspirates, the cell suspension was added with one volume of complete culture media and then centrifuged at 980 rpm for 5 min to concentrate the cells. The cell pellets were resuspended with 5 ml of complete Dulbecco's modified eagles medium (DMEM), then layered over, histopaque-1077 (Sigma) and centrifuged at 2500 rpm for 30 minutes. Mononuclear cells were collected from the interface of Ficoll obtained by gradient centrifugation and washed with  $\text{Ca}^{2+}$  and  $\text{Mg}^{2+}$  free Dulbecco's phosphate buffer saline (DPBS).

The nucleated cells collected were washed with two volumes of DPBS and were then centrifuged at 1500 rpm for 10 min (Fig. 1). The cell count and viability was done after addition of Trypan blue dye in the automatic cell counter and MTT analysis in spectrophotometer. The cells were then seeded in  $1 \times 10^6$ /ml concentration in a T-25 flask. The adherent cells in the flask were maintained in Dulbecco's modified eagles medium-low glucose containing 15% fetal bovine serum (FBS), 1% antibiotic mixture of 100 units/ml penicillin-G and 100  $\mu\text{g}/\text{ml}$  streptomycin (Invitrogen/Gibco) at 37 °C in a humidified atmosphere of 5%  $\text{CO}_2$  and 95% air. Non-adherent cells were removed after 72 hrs of cell seeding. Media was added every 3 to 4 days once until attaining confluence.

After 18-20 days, the flask became confluent and was passaged. Culture media was removed, and cells were treated with trypsin-EDTA solution (0.25 % Trypsin and 1mM EDTA (Gibco)) for 5 minutes at 37 °C to detach cells from the flasks. The Trypsin-EDTA activity was stopped by adding equal volume of complete media, and the media with cells was collected in a centrifuge tube, centrifuged at 4 °C, 1500 rpm for 6 min. The supernatant was removed and the cell pellet was collected and placed in a T-75 flask. Third passage cells were used further for cell differentiation studies and *in vivo* experiments (Fig. 2).

### Preparation of IGF-I

Insulin-like growth factor I was used as a bio-stimulator for this study. Recombinant human IGF-I (Sigma) was used for this purpose. As the  $t_{1/2}$  (half-life) of the free IGF-I is very less, so it was reconstituted in 0.1% Bovine serum albumin (BSA) and phosphate buffer saline for its longer duration of action. The concentration used in this study was 234.74 ng/0.5 ml of IGF-I.

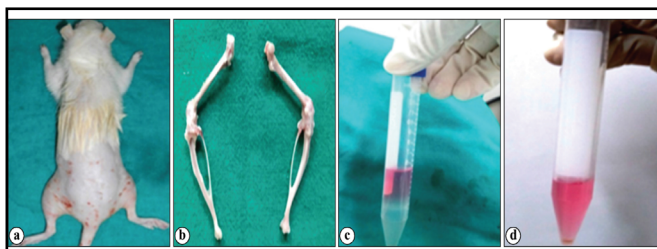


**Fig. 1.** Collection of bone marrow from rat (a) Aseptic site preparation, (b) Collection of femur and tibia (c) Stratified layer of bone marrow after gradient centrifugation (d) Mono and polymorphonuclear cell pellet.

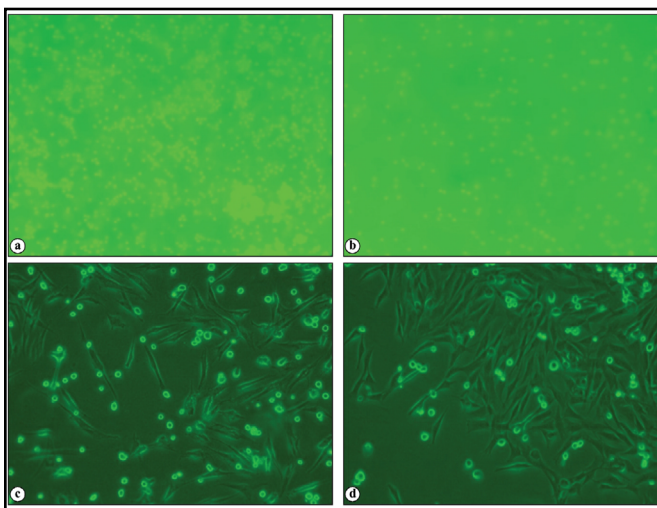


**Fig. 2.** Rat bone marrow derived mesenchymal stem cell culture. (a) P0 day 3; (b) P0 day 14; (c) P0 day 21; (d) Confluent P3.

### *Sciatic nerve crush injury*

Using standard aseptic surgical procedures, intraperitoneal xylazine and ketamine (@ 3 mg/kg and 30 mg/kg, respectively) were administered. Anaesthetized animals were approached caudo-laterally over left hind limb in order to gain access to peripheral sciatic nerve. At the back of the thigh, one longitudinal cutaneous incision was made followed by sciatic nerve exposure through a crush window which was created by dissecting along a plane between the muscle bellies of biceps femoris and semitendinosus muscles. The left sciatic nerve was crushed for ninety seconds using the tip (3mm) of curved haemostatic forceps, and the compression strength was calibrated at the second locking position. Scaffold of size 20 mm × 5mm was wrapped around the crushed nerve site. A 3-0 vicryl suture was utilized to suture muscle followed by 2-0 polyamide for sealing the skin (Fig. 3).

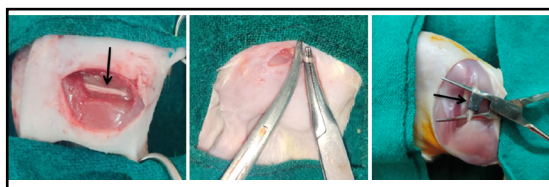


**Fig. 3.** (a) Exposing Sciatic nerve (black arrow- showing sciatic nerve); (b) Creation of sciatic nerve crush injury using hemostat calibrated at second locking position and (c) Scaffold implantation (black arrow- showing Collagen+Polycaprolactone+ Multiwalled Carbon Nanotubes Scaffold).

In groups supplemented with IGF-I, first instillation was done intra-operative at the site of crush injury. Later doses were repeated at 3, 7, 14, 21- and 28-days interval intramuscularly at the operative site.

The animals were housed individually after recovering from anaesthesia, with antibiotics, analgesics, and antiseptic ointment applied topically. The animals were euthanized according to standard guidelines at 30-, 60- and 90-days post scaffold treatment, and the tissue of interest for study gastrocnemius muscle and sciatic nerve were collected and processed for various analysis.

### *In vitro scaffold testing*

#### *Scanning electron microscopic surface study of the neural scaffold*

The samples were fixed in 2.5% glutaraldehyde at 4 °C for two hours. Following a PBS wash, samples were dehydrated in increasing percentages of alcohol for 10 minutes at a time, including 30%, 50%, 70%, 80%, 90%, and 100%. Initially, supracritical drying was accomplished using hexamethyldisilazane (HMDS) for 10 minutes. Following air drying and gold sputtering, the samples were scanned using a scanning electron microscope. High resolution images were then captured using secondary electron imaging mode at 1000X with 15-20 kV electron beams [5]. Working depth was maintained at 7–10 mm.

#### *Mechanical strength of the neural scaffold (Tensile strength)*

Using a low load universal tensile testing machine, the mechanical characteristics of the scaffolds were identified. The mechanical test adhered to ASTM standard D368. According to the ASTM standard, uniaxial tensile testing was performed on 15× 5 mm strips of each type of scaffold with a gauge length of 2 mm while maintaining a strain rate of 0.1 mm/s. The experiment was carried out in triplicates for each kind of scaffold in order to calculate the Young's modulus.

#### *Electrical property of the neural scaffold*

Scaffold's electrical property was measured in form of I-V characteristics in which specific voltage was applied to 1 × 1 cm scaffold and current was measured. The experiment was performed at room temperature in triplicates for each scaffold. The following equation was used to calculate the resistivity of the scaffolds using I-V characteristics:

$$\rho = V \times A / I \times L$$

Where,  $\rho$  represents desired resistivity,  $V$  represents voltage applied,  $A$  represents the electrode area,  $I$  represents the obtained current and  $L$  represents the distance between electrodes. The obtained resistivity was used to calculate the conductivity. The following equation was used to calculate the conductivity:

$$\sigma = 1/\rho$$

### *Degradation of neural Scaffold*

To check the biodegradability of the scaffolds, they were subjected to degradation test in a modified buffer system, simulating the biochemical composition of the tissue fluid. These scaffolds were expected to encounter *in vivo* conditions. Degradation of the scaffolds was checked in single modified buffer system, namely, mPBS which contains collagenase and lipase. Each type of scaffold (L: 20 mm x W: 5 mm x H: 1 mm) was immersed in the mPBS individually and incubated for 60 days at 37 °C in a sterilized environment. Every 5 days of interval, old mPBS were replaced with fresh mPBS and scaffolds were washed thoroughly with deionized water, air dried and weighed. The percent weight loss of the scaffolds was plotted against time (in days).

### *Diamidino-2-phenylindole (DAPI) Staining*

A stem cell-seeded composite random polymeric neural scaffold made of PCL, collagen and MWCNT was preserved with 4 % paraformaldehyde at 4 °C for 30 minutes. Following two PBS washings, the scaffolds were treated with 4, 6-diamidino-2-phenylindole for two minutes. The scaffolds were then again cleaned twice with PBS. Fluorescent microscopic visualisation revealed blue immunofluorescence because of stem cells' DAPI-labelled nuclei.

### *Physical and Neurological Examination*

#### *Pinch Test (Functional Assessment of Reinnervation)*

Recovery of sensory function was being analysed using pinch test. A gentle pinching stimulus was delivered to the skin of the left hind limb, from the toe to the knee joint, with conventional forceps, until a strong withdrawal reflex was noticed and according to this observation grading was done from 0 to 3: 0 = no withdrawal response, 1 = response to stimulus above the ankle, 2 = response to stimulation distal to the ankle in the heel/plantar region, and 3 = response to stimulation in the metatarsal region [6] [7].

#### *Toe-spread test*

The abduction and extension reactions of the toes were measured for the toe-spread test, which is a motor recovery indicator. The results were rated on a scale of 0 to 3: 0 = no toe movement, 1 = some sign of toe movement, 2 = toe abduction, and 3 = toe abduction with extension.

#### *Sciatic functional index (SFI)*

The functional state of the animals was measured at regular intervals using the sciatic functional index (SFI) [8]. Pre-operatively, 30 days, 60 days, and 90 days post-surgery, a walking track analysis was undertaken. The rat's hind feet were painted with nankin ink, and the animals were placed in a walking route to leave their imprints. On the Test (E) and the control side (N), the lengths of the 3<sup>rd</sup> toe to heel (PL), 1<sup>st</sup> to 5<sup>th</sup> toe (TS), and second toe to fourth toe (IT) was measured in each rat. The following formula was utilized to compute the SFI in each animal. The SFI revolves around 0 for normal nerve function and about -100 for total nerve impairment in general.

$$SFI = -38:33 (EPL - NPL) / NPL + 109:5 * (ETS - NTS) / NTS + 13:33 (EIT - NIT) / NIT - 8:8$$

#### *Toe out Angle (TOA)*

In rats, functional improvement of the sciatic nerve is thought to be associated with external rotation of the leg. The TOA, which is defined physiologically from the calcaneus to the tip of the third digit, is the angle, measured in degrees, between the direction of progression and a reference line. The rats were placed on a 15x15x3 cm acrylic glass sheet to measure TOA. The plantar surface of the animals' paws was photographed with a camera placed beneath the clear base plate [9]. Angles were measured and recorded.

#### *Biochemical Parameters*

Blood was collected from the orbital plexus of rats using capillary tubes and two ml of blood was drawn at 30<sup>th</sup>, 60<sup>th</sup> and 90<sup>th</sup> day postoperatively. For C - reactive protein estimation blood was collected at 7-, 14- and 21-days interval. Serum separation was done in order to quantitative inflammatory mediators like C-Reactive Protein (CRP) using rat-CRP ELISA kit (Sigma) and other biochemical parameters Serum Glutamate Pyruvate Transaminase (SGPT), Serum Glutamic-Oxaloacetic Transaminase (SGOT), creatinine,

blood urea nitrogen (BUN) and blood glucose using standard commercially available kits. Biochemical analysis was done in order to rule out any possibilities of *in vivo* systemic toxicity related to the use of scaffold.

### Gross and Muscle morphometric Analysis

After euthanizing the animal on day 30/60/90 days post scaffold treatment, the gastrocnemius muscle were excised out to access the weight of the gastrocnemius muscle in the experimental (E) and control (C) limbs. Individual animal's E/C ratio of experimental limb (left limb) gastrocnemius muscle to normal limb (right limb) muscle were calculated for weight and compared to other groups.

### Histopathological observation

Gastrocnemius muscle and sciatic nerve were collected on 30<sup>th</sup>, 60<sup>th</sup> and 90<sup>th</sup> days interval for histopathological evaluation. Samples were fixed in 10% neutral buffered formalin. The samples were further processed for paraffin embedding technique to get 5 micron thick paraffin section. The sections were stained by Hematoxylin and Eosin stain (H&E) to evaluate the regeneration process of muscle and nerve. Sections were also stained with Masson's Trichrome for demonstration of fibro-proliferation and collagen deposition in regenerated muscle and nerve tissue at different intervals of the experiment.

The sections of gastrocnemius muscle were graded from 0 to 3 based on whether or not there were atrophic or degenerative alterations present where 0 denotes Intense, 1 moderate, 2 mild changes while 3 denotes absence of any changes. The sections of sciatic nerve were graded from 0 to 3 based on whether or not there were myelinoclasia and vascular degeneration, Wallerian degeneration (myelin and axonal breakdown), myelin formation (neomyelination) present where 0 denotes Intense, 1 moderate, 2 mild changes while 3 denotes absence of any changes.

### Relative expression of different genes by Real Time PCR

Sciatic nerve samples were harvested and preserved in RNA Later (Sigma) at -80°C post euthanization. The relative mRNA expression profile of three different genes namely neuropillin-1 (NRP-1), neuropillin-2 (NRP-2) and GAP-43 (Growth Associated Protein-43) was performed using DyNAmo SYBR green (Thermo Scientific, USA) and Real Time qPCR machine (Bio-rad, USA) at 30<sup>th</sup>, 60<sup>th</sup> and 90<sup>th</sup> days postoperatively.  $\beta$ -actin was kept as housekeeping gene. Primers used in the study are mentioned in Table 2.

### Scanning Electron Microscopic evaluation of nerve

SEM was used to examine the surface morphology of the left sciatic nerve crush site in one randomly chosen rat from each group on days 30, 60, and 90. Following animal sacrifice, the specimens were kept in 2.5% glutaraldehyde buffer. At the injury site's centre, the preserved samples were divided into two sections for longitudinal and transverse scanning. The samples were examined using a scanning electron microscope (Jeol JSM 6610 LV type) with the proper acceleration voltage and magnification range [10].

### Statistical analysis

All the data were statistically analysed using Statistical Program for Social Sciences (SPSS v.16). One way ANOVA was done to compare the means at different time intervals among different groups. Repeated measures ANOVA were performed for comparing the mean values between different time intervals within a group. Kruskal Wallis Test was done to analyse the non-parametric data within the group at different time points. The non-parametric data among the groups at different time intervals were analysed by Wilcoxon signed rank test.

A value of  $P < 0.05$  (\*) was considered statistically significant while  $P < 0.01$  (\*\*) was considered to be statistically highly significant. All the graphs were prepared in Graph Pad Prism (Version 5).

**Table 2.** Primers used for quantitative real time PCR

Gene	Primer Pairs (5'-3')	Annealing temp (°C)	Amplicon size (bp)
NRP-1	F-GGAGCTACTGGGCTGTGAAG	58	135 bp
NRP-1	R-CCTCCTGTGAGCTGGAAGTC		
NRP-2	F-GCGCAAGTTCAAAAGTCTCCT	60	216 bp
NRP-2	R-TCACAGCCCAGCACTTC		
GAP-43	F- CAGGAAAGATCCCAAGTCCA	58	207 bp
GAP-43	R-GAACGGAACATTGCACACAC		
$\beta$ -actin	F-TATTGGCAACGAGCGG	60	54 bp
$\beta$ -actin	R-CGGATGTCAACGTCAC		

## Results

### *In vitro scaffold testing*

#### *Scanning electron microscopic surface study of the neural scaffold*

Scanning electron microscopic surface morphology of Collagen + PCL + MWCNT scaffold revealed that the scaffold has been constructed without the use of an electric field, so the cross-sectional surface of the scaffolds containing MWCNTs had a rough surface and a dispersed distribution of MWCNTs was observed (Fig. 4a; 1000X).

#### *Mechanical strength of the neural scaffold (Tensile strength)*

Since PCL in scaffold provides elastomeric extension, but it was demonstrated that the maximum extension (strain) was evident following reinforcement with MWCNT which significantly increased the scaffolds' ability to support loads. The Young's Modulus (E) of the Collagen + PCL + MWCNT was found to be  $141 \pm 3.8$ .MPa.

#### *Electrical property of the neural scaffold*

Due to their high electrical conductivity (1000 S/m in the longitudinal and 150 S/m in the transverse axis, respectively), CNTs have been useful in supplying electrical conductivity in PCL-based scaffolds. In Collagen + PCL + MWCNT scaffold, the electrical conductivity in the direction of alignment was 0.000035 ( $\pm 0.0000049$ ) S/m. These findings show that the scaffolds can be given greater conductivity, which stimulates the differentiation of neurons, by strengthening the MWCNTs within the polymeric matrix.

#### *Degradation of neural Scaffold*

Collagen and PCL are well known for degrading biologically. By weighing the scaffolds at predetermined intervals, the degradation of the scaffold was identified. After the fifth day, it was later discovered that MWCNT-containing scaffolds deteriorated more quickly and was found to be  $41.1 \pm 2.2\%$  after 60 days.

#### *Diamidino-2-phenylindole (DAPI) Staining*

After 4 hours and 14 days of nuclei staining with DAPI, the cell attachment revealed proliferating cells on and into the porous area of the scaffold. Additional *in vivo* effects of stem cells would be positive evidence of increased healing and cell proliferation. The proliferating cells with expanded cytoplasm displayed a blue cytoskeleton (Fig. 4b).

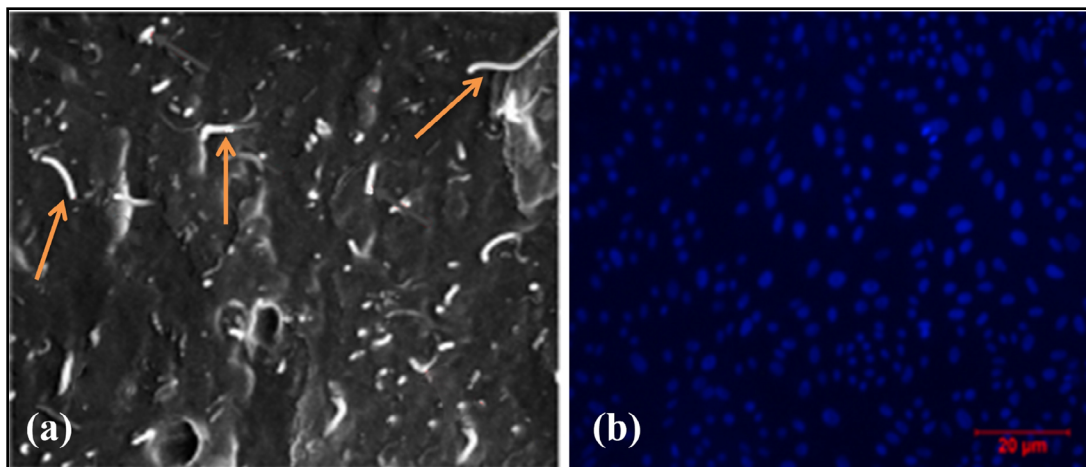


**Fig. 4.** (a) SEM images of Collagen + Polycaprolactone + MWCNT (orange arrow: carbon nanotubes) scaffold (X1000); (b) DAPI staining of rBM-MSCs in cytoskeleton of scaffold.

*Physical and Neurological Examination*

*Pinch Test (Functional Assessment of Reinnervation)*

Pinch test revealed no significant difference among different groups at day 0 (Fig. 5). Group A showed high pain more for than other groups upto 90 postoperative days. The mean score was almost higher at every interval in case of group E when compared with other groups. Pain score was recovered significantly during the three months study except in the control group. However, in other groups changes were insignificant.

*Toe-spread test*

The mean ± SE values of different treatment groups is shown in Fig. 6. In control group A, functional recovery remained significantly lesser (p<0.05) than the base value during the entire period of study. Statistically significant difference (p<0.05) was observed in group E at day 90.

*Sciatic functional index (SFI)*

Sciatic function index of animals of different treatment groups are shown in Table 3. In group A, functional recovery remained significantly lesser (p<0.05) than the base value during the entire period of study. No significant difference was observed among subgroups at day 0 and day 30. While significant changes (p<0.05) were observed in group E and group D at day 60 and 90. In groups A, B and C, sciatic function index remained significantly lower (p<0.05) than the base values score upto 60 days. Comparison among the different groups and subgroups showed a significant functional recovery in group D and E from group A 60<sup>th</sup> day onwards.

*Toe out Angle (TOA)*

The mean ± SE values of toe out angle of animals of different treatment groups are shown in Table 4. The angle between normal and experimental feet is calculated by TOA analysis. Recovery in toe out angle (TOA) remained significantly lesser (p<0.05) in group A during entire period of study. No significant difference was observed among different subgroups at day 0. Significant changes (p<0.05) were observed in group E at day 30. On day 90, highly significant changes (p<0.01) were observed in the group E and D.

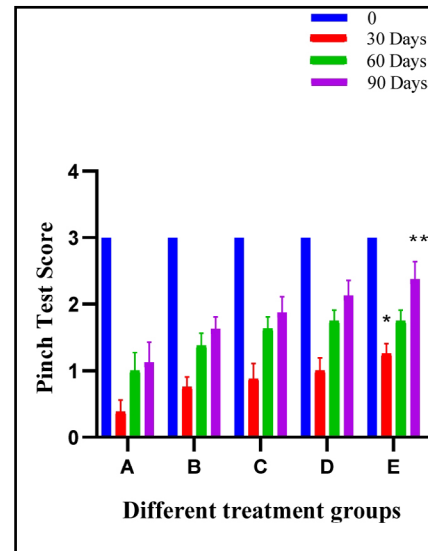


**Fig. 5.** Histogram showing Pinch Test of different treatment groups at various time intervals.

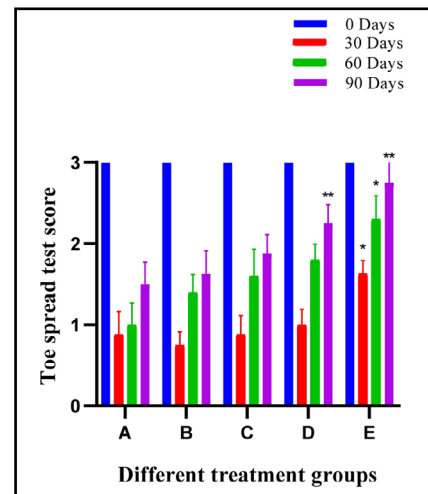


**Fig. 6.** Histogram showing Toe Spread Test of different treatment groups at various time intervals.

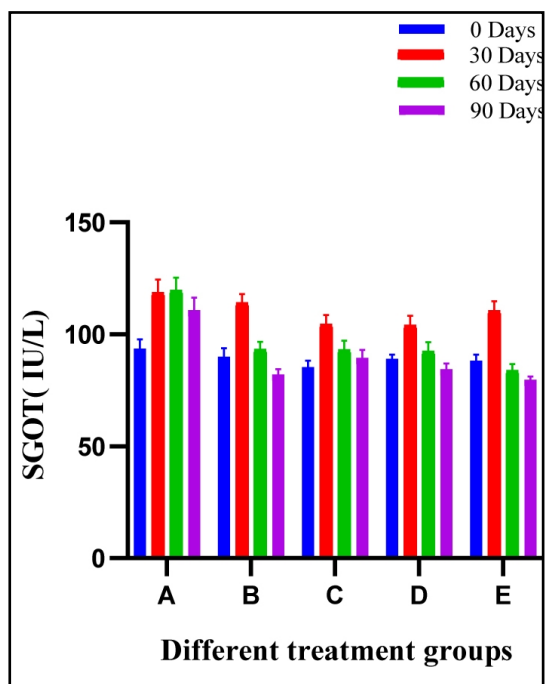
**Table 3.** Sciatic Function Index (SFI) of different treatment groups at various time intervals. \*Mean value differ significantly at P<0.05 within group; \*\*Mean value differ significantly at P<0.01 within the group

Groups	Pre	Day 30	Day 60	Day 90
A	-2.13 ± 1.1	-93.74 ± 2.64	-89.18 ± 1.28	-84.48 ± 1.31
B	-5.15 ± 1.2	-93.08 ± 1.50	-79.71 ± 2.48	-66.9 ± 1.94
C	-5.09 ± 1.5	-91.68 ± 1.79	-78.79 ± 1.48	-64.55 ± 2.33
D	-4.25 ± 2.9	-89.06 ± 2.10	-77.33 ± 2.42	-60.48 ± 2.37**
E	-8.02 ± 1.1	-92.15 ± 1.6	-76.52 ± 1.53*	-41.79 ± 2.34**

**Table 4.** Toe Out Angle (TOA) of different treatment groups at various time intervals. \*Mean value differ significantly at  $P < 0.05$  within group; \*\*Mean value differ significantly at  $P < 0.01$  within the group

	Pre	Day 30	Day 60	Day 90
	14.18 ± 2.1	58.44 ± 2.09	48.66 ± 1.05	42.99 ± 0.90
	7.99 ± 1.3	52.84 ± 1.66	38.26 ± 1.28	32.00 ± 1.98
	12.9 ± 0.6	51.21 ± 1.04	35.27 ± 1.50	30.69 ± 1.35
	7.6 ± 1.6	50.95 ± 1.48	29.65 ± 2.11	20.04 ± 1.66
	8.2 ± 2.0	49.05 ± 0.70*	25.90 ± 2.43**	18.27 ± 1.28**

**Fig. 7.** Histogram showing SGOT (IU/L) values of different treatment groups at various time intervals.



### Biochemical Parameters

#### Serum Glutamic-Oxaloacetic Transaminase

Biochemical analysis was performed to check if any systemic effect of the scaffold is there. In SGOT analysis, no significant difference was observed between different groups at various intervals in comparison with the pre value of the trial. In panoramic view the SGOT ranges were within clinically acceptable limit. The mean ± SE values of SGOT of animals of different groups are shown in Fig. 7.

#### Serum Glutamate Pyruvate Transaminase

In SGPT estimation, no significant difference was observed between groups at various intervals in comparison with the pre value of the trial and conclusively the SGPT ranges were within clinically acceptable limits. The mean ± SE values of SGPT of animals of different groups are shown in Fig. 8.

#### Creatinine

In serum creatinine analysis, no significant difference was observed between groups at various intervals in comparison with the pre value of the trial and conclusively the creatinine ranges were within clinically acceptable limits. The mean ± SE values of the creatinine of animals of different groups are shown in Fig. 9.

**Fig. 8.** Histogram showing SGPT (IU/L) values of different treatment groups at various time intervals.

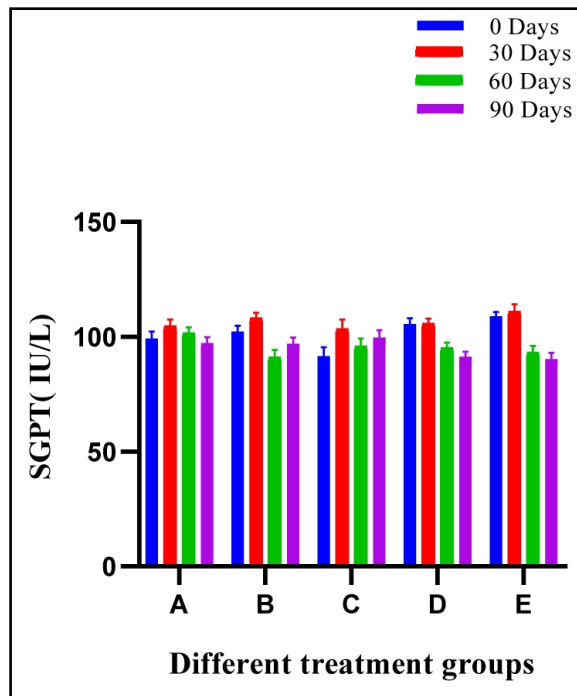
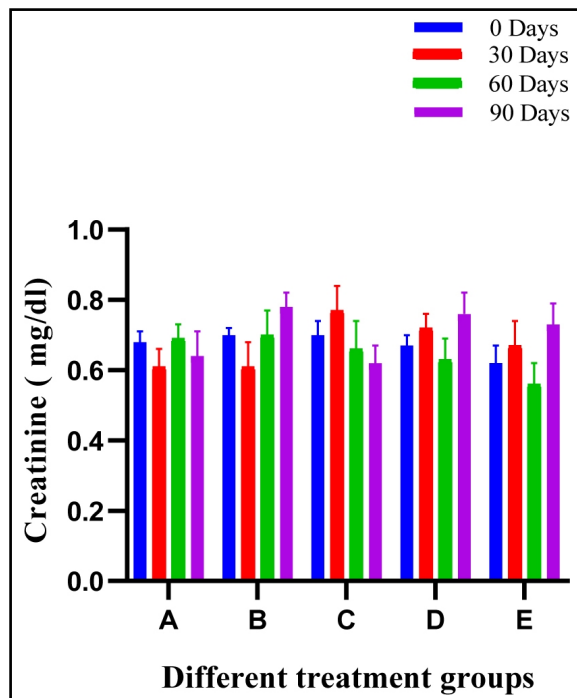


**Fig. 9.** Histogram showing creatinine level (mg/dl) of different treatment groups at various time intervals.



#### *Blood Urea Nitrogen (BUN)*

No significant difference between groups at various intervals was observed. In panoramic view the, BUN ranges were within clinically acceptable limits. The mean  $\pm$  SE values of BUN of animals of different groups are shown in Fig. 10.

#### *Blood Glucose*

In blood glucose estimation, significant difference ( $p < 0.05$ ) was observed in group C and E at day 30 in comparison with day 0 of the study. No significant difference was observed between groups at 60- and 90-days intervals in comparison with the pre value of the trial. The mean  $\pm$  SE values of blood glucose of animals of different groups are shown in Table 5.

**Fig.10.** Histogram showing blood urea nitrogen level (mg/dl) of different treatment groups at various time intervals.

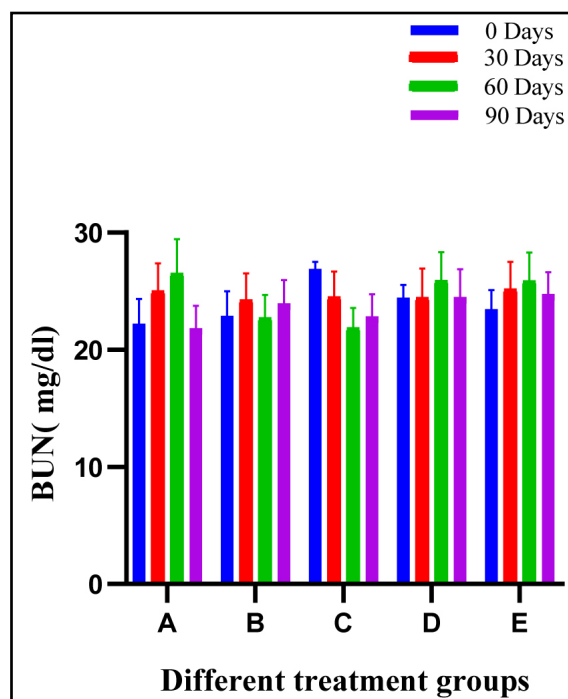


**Table 5.** E/C ratio of weight of different treatment groups at various time intervals. \*Mean value differ significantly at  $P < 0.05$  within group; \*\*Mean value differ significantly at  $P < 0.01$  within the group

Groups	Pre	Day 30	Day 60	Day 90
A	1.0 ± 0.01	0.302 ± 0.02	0.357 ± 0.02	0.517 ± 0.03
B	1.0 ± 0.03	0.390 ± 0.01	0.538 ± 0.02	0.6 ± 0.01
C	1.0 ± 0.02	0.458 ± 0.01	0.527 ± 0.02	0.614 ± 0.02
D	1.0 ± 0.02	0.495 ± 0.02**	0.546 ± 0.02	0.674 ± 0.02**
E	1.0 ± 0.01	0.532 ± 0.02**	0.689 ± 0.02	0.745 ± 0.01**

*C - reactive protein*

In serum C - reactive protein estimation, CRP levels were increased in all groups post crush injury and scaffold implantation and the high levels remained upto 7 days in all groups except in group A where it further increased till day 14. Highly significant ( $p < 0.01$ ) changes were observed in Group B and E while significant changes ( $p < 0.05$ ) in terms of CRP level were noticed in group C and D at day 30. The CRP levels raised upto two-fold comparing to its pre- value of the trial in almost all groups at day 7. No significant changes were seen at day 14 and 21 in group B, C, D and E. The mean ± SE values of the C-reactive protein values of animals of different groups are shown in Table 6.

*Gross and Muscle morphometric Analysis*

Grossly muscle of group A was dull, a little paler, lustreless muscle fascia and of low muscle mass. Muscle belly and tendinous part showed not much difference in terms of thickness. Group B and C almost showed similar physical appearance just differed in muscle masses, group B and C had more muscle mass than group A. In group D and E bright pink muscle, shiny muscle fascia with good muscle mass and also muscle belly to tendon thickness was quite appreciable (Fig. 11).

E/C ratio of gastrocnemius weight remained significantly lesser ( $p < 0.05$ ) in group A during entire period of study. At day 30 significantly higher ( $p < 0.01$ ) changes were appreciated in group E and D when compared with control group A. Non-significant ( $p > 0.05$ ) findings among all groups can be seen at day 60 of the study. At day 90 of the study highly significant ( $p < 0.01$ ) changes were observed in group E followed by group D. The mean  $\pm$  SE values of E/C value of muscle weight of animals of different groups are shown in Table 7.

*Histopathological observation*

In control group A, multiple areas of hyalinisation indicating the degenerating myofibers were evident. Hyalinisation was indicated by highly eosinophilic homogenous mass within the muscle fibre. Striations were absent and marked atrophic changes were present in the section. Vacuoles were present along with muscle shrinkage creating increased space between myofibers. Neovascularisation, hypertrophic changes, and slight myxomatous changes, muscle oedema were seen in focal areas of the samples (H&E 20X). Fibroblastic infiltration was evident in masson's trichrome section (MT 20X). The mean  $\pm$  SE values of gastrocnemius healing score of animals of different groups are shown in Table 8 and Fig. 12.

In group B and C, marked number of myocytes showed mild to moderate degenerative changes with hyaline degenerative changes. Slight amount of fatty infiltration was also seen in the tissue sample of certain animals. In group D and E apparently healthy areas with normal histology were present. Maintenance of normal anatomic structures with absence of any hyaline or fatty degenerative changes was evident. However, area near to neuromuscular junction showed some focal degenerative changes. Some peripheral hyaline changes were seen, but other areas remained normal. Strong fibro-proliferative changes were seen among sections of Masson's Trichrome (MT 20X).

Groups	Pre	Day 7	Day 14	Day 21
A	335 $\pm$ 61	721 $\pm$ 62	797 $\pm$ 78	602 $\pm$ 53
B	287 $\pm$ 45	798 $\pm$ 51**	338 $\pm$ 54	401 $\pm$ 51
C	322 $\pm$ 54	802 $\pm$ 61*	427 $\pm$ 63	414 $\pm$ 62
D	329 $\pm$ 71	795 $\pm$ 68*	346 $\pm$ 63	474 $\pm$ 59
E	292 $\pm$ 65	834 $\pm$ 74**	389 $\pm$ 71	375 $\pm$ 58

**Table 6.** C-Reactive Protein ( $\mu\text{g/ml}$ ) value of different treatment groups at various time intervals. \*Mean value differ significantly at  $P < 0.05$  within group; \*\*Mean value differ significantly at  $P < 0.01$  within the group

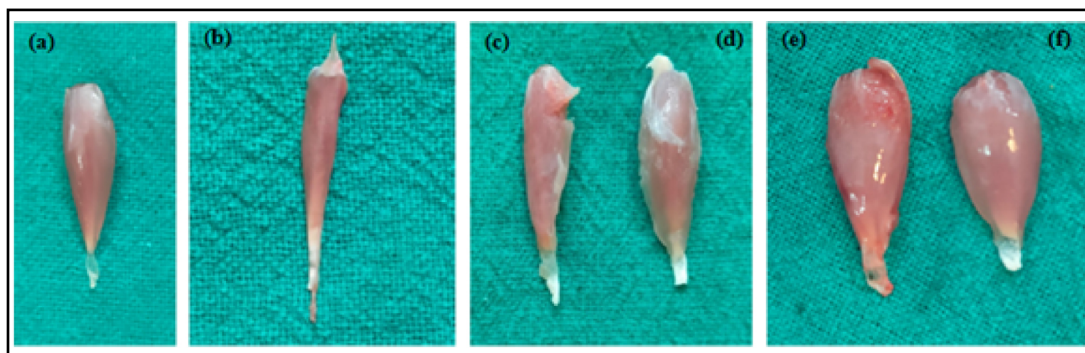


**Fig. 11.** Gross Muscle atrophy post sciatic crush and relative muscle gain post treatment in group various groups (a) Normal (b) Group A (c) Group B (d) Group C (e) Group D and (f) Group E.

**Table 7.** Mean  $\pm$  SE of Blood Glucose (mg/dl) of different treatment groups at various time intervals. \*Mean value differ significantly at  $P < 0.05$  within group; \*\*Mean value differ significantly at  $P < 0.01$  within the group

Groups	Pre	Day 30	Day 60	Day 90
A	73.4 $\pm$ 2.5	72.25 $\pm$ 3.68	68.95 $\pm$ 2.39	80.16 $\pm$ 3.66
B	82.26 $\pm$ 2.6	72.97 $\pm$ 4.09	76.98 $\pm$ 4.05	81.67 $\pm$ 3.29
C	71.59 $\pm$ 3.11	52.46 $\pm$ 2.54*	76.73 $\pm$ 2.47	72.98 $\pm$ 2.91
D	71.8 $\pm$ 2.3	78.57 $\pm$ 3.62	79.62 $\pm$ 2.47	73.69 $\pm$ 2.95
E	76.89 $\pm$ 2.9	53.71 $\pm$ 3.38*	85.2 $\pm$ 2.12	75.15 $\pm$ 2.74

**Table 8.** Gastrocnemius recovery score of different treatment groups at various time intervals. \*Mean value differ significantly at  $P < 0.05$  within group; \*\*Mean value differ significantly at  $P < 0.01$  within the group

Groups	Pre	Day 30	Day 60	Day 90
A	3.0 $\pm$ 0.0	0.625 $\pm$ 0.18	0.625 $\pm$ 0.18	0.75 $\pm$ 0.16
B	3.0 $\pm$ 0.0	0.625 $\pm$ 0.18	0.875 $\pm$ 0.12	1.5 $\pm$ 0.19
C	3.0 $\pm$ 0.0	0.75 $\pm$ 0.16	0.875 $\pm$ 0.12	2.0 $\pm$ 0.19
D	3.0 $\pm$ 0.0	1.0 $\pm$ 0.0	1.125 $\pm$ 0.23	2.125 $\pm$ 0.23
E	3.0 $\pm$ 0.0	1.0 $\pm$ 0.0	1.625 $\pm$ 0.18	2.625 $\pm$ 0.18

In group A, intense myelinoclasts and vacuolar degeneration was seen in majority of animals, while the others were showing a moderate amount of myelinoclasts. The degenerative changes were indicated by presence of more cellularity in the sections. Four animals showed moderate amount of Wallerian degeneration, while in other animal intense degenerative changes were observed. Weak presence of myelin, sparsely distributed in the sections, was noticed in the group. Increased number of inflammatory cells along with degeneration were present. Vacuolations were also seen more frequently indicating the accumulation of the oedematous fluid. Large number of giant cells of varying sizes was evident in H&E sections (Fig. 13). The mean  $\pm$  SE values sciatic nerve recovery score of animals of different groups are shown in Table 9.

In group B, C and D, some normal areas along with degenerated areas were observed. Nerve fibers were intact; less giant cell number; less inflammatory changes were present, mild amount of cellular infiltration was present. In group E, in about three animals' only mild change of vacuolations and myelinoclasts was evident while moderate myelinoclasts was observed in other subgroups. Level of Wallerian degeneration was graded as mild.

Comparison among different group at day 30, 60 and 90 revealed no significant difference in terms of myelinoclasts, Wallerian degeneration and myelin formation except for group E where significant changes ( $p < 0.05$ ) were evident in all the stained sections of H&E, Masson's Trichrome (Fig. 13).

*Relative expression of different genes by Real Time PCR*

Relative expression of NRP-1, NRP-2 and GAP-43 genes was quantified by real time PCR and results are shown in Table 10 and Fig. 14. At day 90, expression profile of group B, C were lower in comparison to control group A, while a higher value of expression was seen in group D and E. Relative mRNA expression of NRP-2 showed a trend similar to NRP-1 where a lower value of expression was seen in group B, C while a higher value of expression was seen in group D and E. The profile of GAP-43 gene transcripts in this study on comparison with control group A, showed a higher expression. Overall, the relative mRNA expression of subgroups of group E dominated all the other groups and had a higher mean score.

**Fig. 12.** Gastrocnemius muscle sections: (a-c) H&E staining (20X) of groups A, B, C, D and E at different time intervals (d30; 60; 90); (d) Masson's Trichrome staining (20x) of groups A, B, C, D and E at 90 days interval.

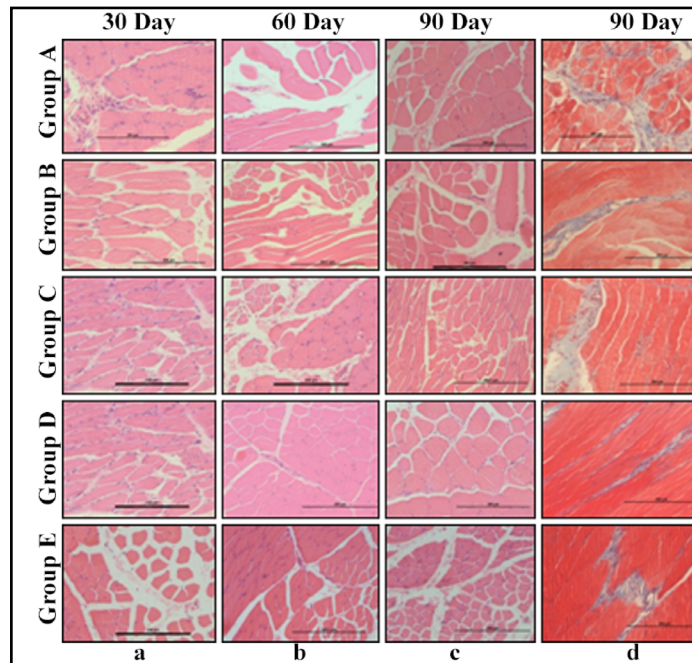


**Fig. 13.** Sciatic nerve sections: (a-c) H&E staining (20X) Of groups A, B, C, D and E at different time intervals (d30; 60; 90); (d) Masson's Trichrome staining (20x) Of groups A, B, C, D and E at 90 days interval.

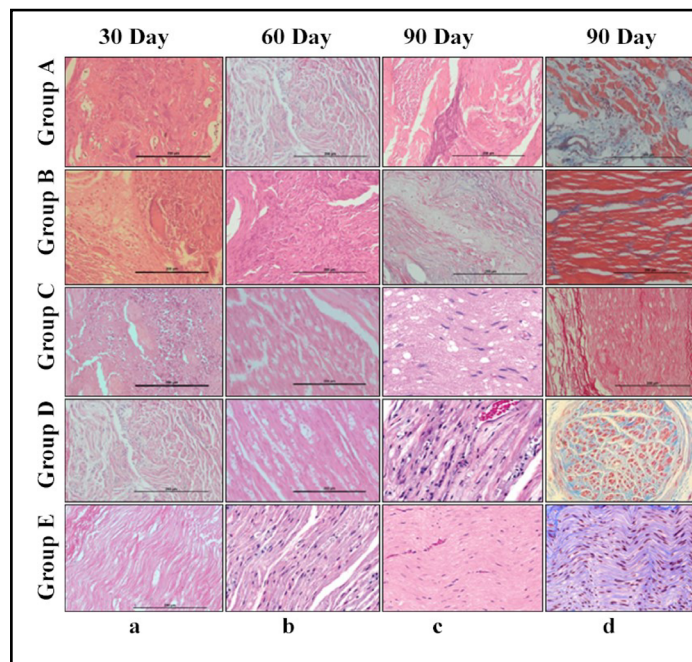


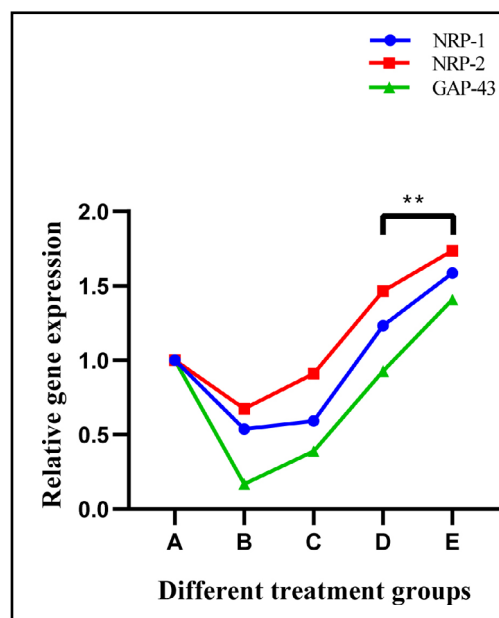
**Table 9.** Sciatic nerve recovery score of different treatment groups at various time intervals. \*Mean value differ significantly at P<0.05 within group; \*\*Mean value differ significantly at P<0.01 within the group

Groups	Pre	Day 30	Day 60	Day 90
A	3.0 ± 0.0	0.625 ± 0.18	0.875 ± 0.29	1.375 ± 0.18
B	3.0 ± 0.0	0.75 ± 0.16	1.625 ± 0.18	1.625 ± 0.18
C	3.0 ± 0.0	0.875 ± 0.12	1.75 ± 0.16	1.75 ± 0.16
D	3.0 ± 0.0	1.0 ± 0.0	1.625 ± 0.18	2.25 ± 0.25
E	3.0 ± 0.0	1.25 ± 0.16	2.0 ± 0.19	2.5 ± 0.19

**Table 10.** Relative expression of NRP-1, NRP-2 and GAP-43 genes in various treatment groups at 90 days post scaffold treatment

Group	NRP-1	NRP-2	GAP-43
A	1	1	1
B	0.538	0.675	0.169
C	0.592	0.911	0.388
D	1.231	1.464	0.926
E	1.585	1.737	1.407

**Fig. 14.** Line diagram showing relative gene expression profile of NRP-1, NRP-2 and GAP-43 at day 90 post scaffold treatment.



*Scanning Electron Microscopic evaluation of nerve*

The scanning electron microscopy of the sciatic nerve sample collected at day 90 was done to assess the orientation of the fibrillar network and surface morphology of the injured nerve. None of the nerve samples showed a completely normal electron microscopic appearance of the sciatic nerve. The longitudinal and transverse sections of the nerve samples were compared with the normal sciatic nerve collected from the contra lateral limb. In group A, smooth fibres with randomly arranged fibrils were noticed. In almost group B, C fibers could be visualized but had a rough surface morphology without any clear demarcation of the fibre when compared to the normal sciatic nerve. In group D, randomly arranged fibrillar network with rough surface morphology similar to group B, C was noticed, whereas in group E radially arranged fibre could be visualized with rough connective tissue network and a surface morphology resembling normal nerve architecture could be visualized but complete healing could not be recorded (Fig. 15).

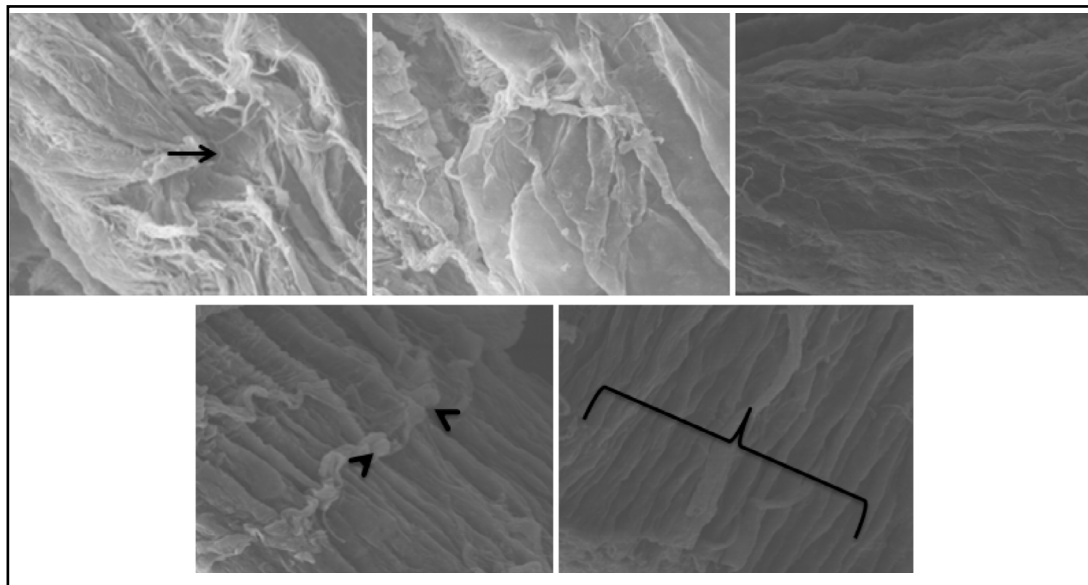


**Fig. 15.** SEM images of rat sciatic nerve of various treatment groups at day 90 (small arrow- Site of injury, arrow head- cell entrapped within fibers, curly bracket- radially arranged fibers in normal orientation and architecture).

## Discussion

The Peripheral Nervous System is made up of an intricate network of ganglia, or clusters of neurons, in the brain and spinal cord. In order to convey sensory messages to and from the spinal cord, these cells communicate with other tissues [11]. The PNS has the capacity to slowly regenerate on its own (axon growth 0.5–1 mm/day); in the event of minor injuries, nerve axons can recover by expanding Schwann cells and macrophages to clear away cellular debris from the damaged side. In order to stimulate and direct the newly formed axon across the injured nerve, Schwann cells penetrate the wound [12]. On the other hand, more severe wounds require surgical repair, frequently involving an autologous nerve implant. While the environment at the injury site is taken into account by extrinsic factors, intrinsic factors that affect PNS regeneration include the extent of the injury and the neurons' capacity to recover through the production of growth factors [11] [12] [13]. In general, tissue engineering and nanotechnology work to develop new materials to hasten PNS recovery because a delay in tissue renewal could result in muscle atrophy.

Insulin-like Growth Factor I is a key neurotrophic factor for the survival and proliferation of motor neurons. According to studies, local IGF-I transgene expression in skeletal muscle following a sciatic nerve lesion enhances muscle differentiation as well as intramuscular neurite development [14]. Following preterm sciatic nerve axotomy, systemic IGF-1 therapy enhances muscle reinnervation, prevents motoneuron mortality, and fosters neurite growth and survival of developing oculomotor neurons [15] [16]. In a mouse ALS model, recent research has demonstrated that retrograde adeno-associated viral administration of IGF-I constructs increases motor neuron survival and slows disease progression [17]. The combination of IGF-I and Glial cell line-derived neurotrophic factor (GDNF) totally rescues rat motor neurons from prolonged glutamate-mediated toxicity in organotypic spinal cord preparations, and IGF-1 potentiates the neurite-promoting activity of GDNF20. As a target derived neurotrophic factor, it is believed that IGF-I itself, or maybe one or more of its signalling pathway mediators, retrogradely transports to motor neurons to promote nerve growth [18].

In cultured neuroblastoma cells and myenteric plexus neurons, IGF-I has been demonstrated to enhance axon outgrowth. In cultured sciatic nerve segments of rat model, insulin, IGF-I, and IGF-II are mitogenic to myelinating Schwann cells [19]. Cheng and coworkers discovered that without IGF-I, axonal myelination does not take place in co-cultured neurons of dorsal root ganglion with Schwann cells. IGF-I injected locally has been proven to speed up axon regeneration after a sciatic nerve crush or freeze injury [20][21]. IGF-I is required for long-term myelination as well as Schwann cell adhesion and ensheathment of axons. Without presence of IGF-I, no myelination occurs [22] [23].

IGF-I plays a factor in encouraging stem cells to take part in the regeneration of neural tissue. Adult forebrain stem cells treated with IGF-1 generate neurons, as evidenced by an increase in multipolar axonal development and the production of the neuronal growth and maturation marker GAP-43 protein [23].

The experimental study was done on seventy-five adult Wistar rats of either sex, divided into five groups. Trial animals were evaluated at 30 days interval for 3 months. Sciatic nerve injury of left limb was created by crushing the left sciatic nerve with 6-inch haemostat pressed up to the second lock position for 90 seconds. The capacity of injured sciatic nerve to regenerate in response to different treatment protocols were evaluated using different parameters, which included clinical parameters like pain, toe expansion score, sciatic function index (SFI), toe out angle (TOA), macroscopic evaluation of gastrocnemius muscle for its weight, microscopic evaluation of gastrocnemius muscle and sciatic nerve, relative expression of genes for three nerve repair markers on day 90 and scanning electron microscopy of the injured nerve.

Following crush injury, the animals showed ataxia, altered gait, dragged the foot, rested on the dorsum of the affected foot, lateral deviation of the hock of the experimental limb

and reduced response to pinch test. The animals positioned the experimental limb outwards from the body, contrary to the normal pattern of putting the legs under the body. The sciatic nerve crush injury model used in the present study has been established earlier for regenerative nerve studies in rats [24] [25] [26] [27] [28]. After creation of nerve injury, animals develop weakness, altered gait and lengthening of foot prints in rats [29]. In the present study the sciatic nerve was made as described by Tiwari and a uniform nerve injury model was established [10].

In the present study clinical parameters including pain, toe spread score; sciatic function index and toe out angle were assessed at 30 days interval. It was found that in all the groups the mean score of pain before injury was 3 indicating fully intact pain pathways for both superficial and deep pain. Immediately after the crush injury the mean score was almost  $\leq 1$ , denoting absence of superficial and deep pain sensation. By day 90<sup>th</sup> the pain score values reached very close to 2.25 but not reached baseline. Pain score was recovered significantly during the three months study except in the control group A. BMSCs has beneficial effects on the healing of sciatic nerve in rats [30].

Toe spread scoring was done after evaluating the abduction and extension reactions of the toes. Significant changes were observed in group E at day 60 and group E and D at day 90. In groups A, B and C, mean scores of toe spread test score remained significantly lower than the base values score upto 60 days. Comparison among the groups showed a significantly higher mean score in group D and E from group A 60<sup>th</sup> day onwards.

Prior to surgery, SFI values in all the groups were near zero. After the nerve transaction, the mean SFI decreased near to - 100 due to the complete loss of sciatic nerve function in all animals. At the end of the study period the statistical analyses revealed that the recovery of nerve function in groups A, B and C, remained significantly lower than the base values score upto 60 days. Comparison among the different groups showed a significant functional recovery in group E and D from group A 60<sup>th</sup> day onwards. The functional recovery was almost higher at every interval in group E when compared with other groups. The SFI analyses showed significant functional recovery in the grafted groups with scaffolds/cells and IGF-I compared to the group A.

The angle between normal and experimental feet was calculated by TOA analysis. On day 90, highly significant changes were observed in group E, D and C. Considerable temporal changes were observed in case of group C, D and E showing good rate of recovery in toe angle. The results showed significantly better angle for the contra lateral foot than the experimental foot in animals implanted with scaffold having Collagen + PCL + MWCNT with BMSCs and IGF-I and it showed a better recovery compared to the control group. Toe out angle in animals treated with autografts and nanofibrous conduit with SCs group showed better recovery compared to the control group [30].

Locomotion is a highly coordinated process that demands exact timing (speed) of impulse conduction to produce coordinated movements. When demyelination occurs as a result of a crush injury, this typical coordination is altered, action potentials are delayed, and regular motions become disorganised. The difficulty of denervated muscles to accept reinnervation has been linked to poor functional recovery following peripheral nerve damage [31]. The demyelination brought on by crush injury may be the source of the impaired coordinated movements observed in the current investigation. According to the sciatic function index, researchers were able to fully recover sciatic nerve injury in rats after 28 days [32], but other researchers have noted significant variations in recovery times, with models of axonotmesis typically requiring three to eight weeks [33] [34] [35] [36]. The various compression devices that were employed to cause the sciatic nerve injury may be the cause of the variations in the recovery times observed in the various trials. In the current study, subgroups of group E and D showed neurorecovery earlier, with mean scores that were similar to baseline values.

Biochemical analysis was done to evaluate the systemic effects of scaffold (hepato or nephrotoxicity). In biochemical analysis no significant difference was observed between groups at various intervals in comparison with the pre value of the trial and conclusively the SGOT, SGPT, BUN and creatinine values were within clinically acceptable limit but in glucose

analysis, significant difference were observed in groups group C and group E at day 30 in comparison with day 0 of the study. The findings might be due to instillation of IGF-I at 1, 4, 7, 14, 21 and 28<sup>th</sup> day in the first month of trial which caused transient lowering of blood sugar for a while. Other changes remained constant for next two months. In a different study similar biochemical findings were obtained while using MWCNT based scaffolds for bone regeneration study in rabbits [37].

Moreover, the biochemical assessment of serum CRP level was performed as a biomarker of inflammation. Highly significant changes were observed in group B and E at day 7. While the serum CRP value increased upto day 14 in case of group A. No significant difference was observed between groups at 14- and 21-day intervals in comparison with the pre value of the trial in group B, C, D and E and conclusively the values were within clinically acceptable limit. Similar findings were reported in sciatic nerve chronic constriction studies in mice [38].

In the present study the ratios of muscle weight of experimental and control gastrocnemius muscle were analysed to assess the functional recovery. It was found that the sciatic nerve crush injury resulted in reduction of muscle weight. This was observed by gross observation of the muscle in live animal during the entire study period and none of the muscle sample reached ratio of 1 by day 90. The study showed significantly better ratio in the animals treated with stem cells compared to other groups and the control group. Considerable temporal changes were observed in case of group B, D and E showing good rate of recovery in gaining muscle mass. The results showed significantly better E/C ratio in group E implanted with scaffold having Collagen + PCL + MWCNT with BMSCs and IGF-I and it showed a better recovery compared to the control group. The muscle weight and the muscle to body weight ratio after sciatic nerve transection reduced significantly [39]. They have also reported that peripheral nerve transection resulted in drastic reduction in the muscle mass when compared to a spinal cord transection model. In a similar study, gastrocnemius muscle weight was compared and it was found that the smallest E/C ratio was obtained by the empty treatment group in which nerve regeneration was never observed while highest E/C ratio was observed in the rats that received the autografts [40].

The bone marrow derived mesenchymal stem cells can differentiate into myelinating cells capable of supporting nerve fibre re-growth and nerve regeneration [41] [42]. The bone marrow derived mesenchymal stem cells are capable of differentiating into Schwann cell like cells both *in vivo* and *in vitro* and induce myelination of regenerated fibers after sciatic nerve injury [43] [44] [45]. In general, the stem cell treated Collagen+PCL+MWCNT group comparatively better score was observed in terms of gastrocnemius muscle weight and volume. This might be due to the early reinnervation to the muscles supplied by the sciatic nerve including muscle which might have enabled the animal to use limb earlier. Some of the therapeutic effect of MSCs is mediated by the paracrine factors secreted by the cells [46] [47]. The secretions by MSCs of soluble factors can alter the microenvironment by trophic activity [48]. Extensive proteomic analyses have revealed that MSCs *in vitro* produce a variety of factors that influences a broad range of biological functions, angiogenesis and secrete neuroregulatory peptides and cytokines with critical role in inflammation and repair [49]. E/C ratio of gastrocnemius muscle weight clearly indicated a significantly better healing in group E compared to other groups.

Gastrocnemius muscle histopathology is used to indirectly assess the status of regeneration of the injured nerve. The muscle is supplied by the sciatic nerve and crush injury would lead to quick atrophy of the muscle as observed macroscopically. After sacrificing the animals, H&E and masson's trichrome section of gastrocnemius muscle were examined for the presence of atrophic and degenerative changes. Specific histological features of a skeletal muscle like striations and multinucleated myofibers were absent, and degenerative changes including angular atrophy, hyalinisation characterised by highly degenerated areas, absence of striations etc were seen in a variable degree in the muscle sections of different groups. The individual sections were scored and scores were compared among the different groups of sciatic nerve injury. Animals of control group A showed maximal muscle atrophy

characterised by multiple areas of hyalinisation indicating the degenerating myofibers, absence of striations with marked atrophic changes, vacuolations, fibroblast infiltration and slight myxomatous changes with muscle oedema. All the treatment group animals showed comparatively better score. Comparison among H&E-stained sections of different groups revealed a higher mean score in group E and D followed by group C and B. However, no significant difference was observed between groups at day 30.

The bone marrow derived mesenchymal stem cells are capable of differentiating into Schwann cell like cells both *in vivo* and *in vitro* and induce myelination of regenerated fibre after sciatic nerve injury [43] [44] [45]. This might be due to the early reinnervation to the muscles supplied by the sciatic nerve including muscle which might have enabled the animal to use limb earlier. High mean score was observed in the stem cell treated Collagen+PCL+MWCNT group where IGF-I was given at committed intervals.

The response of the peripheral nervous system following injury varies with the cause and extent of injury and the different pathological changes depend on the degree of injury. After sciatic nerve injury, Wallerian degeneration occurs in the distal stump consisting of a series of processes, including axonal degeneration, myelin degeneration and disintegration, Schwann cell proliferation, infiltration of macrophages and mast cells, and axonal and myelin debris clearance [50]. Response to injury by nerve fibre is a process of preparing for nerve regeneration. Peripheral nerve regeneration is the process when degenerated axons and myelin are cleared with the establishment of a regeneration friendly microenvironment, after which nascent buds grow from axons proximal to the injury and extend along the regenerative channel to target organs and contact with them to achieve reinnervation of target organ [51]. Histology is a traditional method to evaluate the recovery of regenerated nerves. Nerve regeneration can be indirectly reflected by histomorphological parameters, including myelinated nerve fibre, regenerate axon diameter and myelin sheath thickness. In the present study, histological examination of regenerated nerves was done by conventional H&E staining and Masson' Trichrome. At 30, 60 and 90 days after surgery, sciatic nerve samples were collected. The sciatic nerve showed different levels of regenerative process on day 90 but none of the histological samples showed a completely recovered sciatic nerve. Histopathological scoring of different parameters including myelinoclasts, Wallerian degeneration and formation of myelin were done and mean score of the parameters and an overall histological score was also obtained. Scoring of myelinoclasts showed a better recovery score in the stem cell treated Collagen+PCL+MWCNT scaffold group with IGF-I, i.e group E followed by group D. Wallerian degeneration with presence of digestion chambers and degenerated fibre were less evident in the group E followed by group D. Myelin formation did not differ much among groups. Overall histological score obtained after adding up the individual scores of these parameters were compared among the groups. The results showed a clear evidence of increased regenerative capacity of the stem cell therapy.

In the study where bone marrow derived mononuclear cells were transplanted directly between the ends of a transected sciatic nerve, increased rate and degree of nerve regeneration was observed [52]. The transplanted cells facilitated the process of myelin formation (in terms of both percentage of myelinated fibre and thickness of the myelin rings) and axon regeneration and decreased incidence of degenerative changes. After stem cell therapy, the release of neuro trophic factors may help axonal growth. The differentiation of the stem cells into Schwann-like cells may contribute to myelin reformation and modification of extracellular matrix. Even down regulation of some inhibitory molecules has been shown which could promote and facilitate axonal sprouting [53] [54]. The regeneration of damaged nervous tissue could be initiated by differentiation or transdifferentiation of stem cells into mature neural cells, thus promoting the remyelination of the surviving axons and the restoration of specific connections [55] [56] [57] [58]. The stimulation of endogenous neurogenesis and angiogenesis, the secretions of exosomes, and the activation of endogenous stem cell proliferation, migration and differentiation towards neural cells [59] [60] might have helped healing of injured nerve in stem cell treated animals.

Expression profile of different genes in groups B and C were lower in comparison to control group A, while a higher value of expression was seen in group D and E at day 90. Relative mRNA expression of NRP-2 showed a trend similar to NRP-1 where a lower value of expression was seen in group B and C while a higher value of expression was seen in groups D and E. The profile of GAP-43 gene transcripts in this study on comparison with control group A, showed a higher expression in group E and D, while a lower value of comparison was observed in other groups. Overall, the relative mRNA expression of group E dominated all the other groups and had a higher mean score. Similar findings were observed while treating sciatic nerve injuries of rabbits with stem cells and stem cell conditioned media [61].

The receptors neuropillin-2 (NRP-2) and neuropillin-1 (NRP-1) are part of the well-known class of semaphorins, which are ligand-responsive receptors with a number of subclasses [62]. NRP-1 and NRP-2 individually react to particular semaphorins from subclass 3 secreted proteins that direct axonal growth cone migration to the correct target region during development [63] [64] [65]. The expression of neuropillins in the central nervous system is linked to the development of scar tissue after injury, which is thought to play a significant role in the limiting of regeneration in the central nervous system [66] [67]. In contrast, the production of NRP-2 after nerve injury may promote nerve regeneration in the peripheral nervous system. Prior research had shown that the Schwann cells in the crush site and distal stumps of crushed rodent nerves induced NRP-2 at the messenger ribonucleic acid (mRNA) level [68] [69].

Functional, clinical, and histological research have not revealed any common trends in these genes' expression profiles. This may be explained by the fact that early or after injury, particularly after two weeks, changes in the expression pattern of mRNA occur. A small sample size and inconsistent preservative conditions in the current study's sciatic nerve samples collection could have contributed to the study's inconsistent findings.

The scanning electron microscopy of the sciatic nerve samples collected on various intervals was done to assess the orientation of the fibrillar network and surface morphology of the injured sciatic nerve. None of the sample showed completely normal scanning electron microscopic appearance of the sciatic nerve. Basal lamina of a normal nerve in cross section appeared as distinct ring like structure under fluorescent microscope [69]. Whereas, the ring pattern which was found difficult to distinguish in a damaged nerve fibre. Hence longitudinal section of the nerve samples were compared to the normal sciatic nerve collected from the contra lateral limb. In group A smooth fibre with randomly arranged fibrils were noticed. In subgroups of group B and C, fibre could be visualized but had a rough surface morphology compared to the normal sciatic nerve. In group D, randomly arranged fibrillar network with rough morphology similar to group B and C was noticed, whereas, in group E, a surface morphology similar to normal sciatic nerve could be seen but complete healing could not be recorded. SEM finding indicating a healing pattern was in agreement with the histological and clinical parameters as reported earlier in a study of nucleated marrow cells along with TGF- $\beta$ 1/IGF-1 for cartilage and nerve repair in rabbits [10]. The animals treated with Collagen+PCL+MWCNT along with stem cells and IGF-I i.e group E showed a better healing as assessed by scanning electron microscopy. As a result, the improved functional recovery seen in group E after using the Collagen+PCL+MWCNT scaffold in combination with stem cell therapy and IGF-I may be attributable to the optimization of both the time of the therapy and cell-based treatment.

## Conclusion

In conclusion, *in vitro* seeding of rBMSC on Collagen + PCL+ MWCNT nano-neural scaffold hasten the neuro-regenerative property of the scaffold and infusion of IGF-I at various intervals triggered and accelerated myelination in injured nerves thus helps in enhancing healing and can be used as an alternative strategy for nerve regeneration in peripheral nerve

injuries. Significant recovery was observed in group E, where SFI and TOA just after surgery were  $-92.15 \pm 1.6$  and  $49 \pm 0.70$  and post 90 days were reduced to  $-41.79 \pm 2.34$ , TOA came to  $18.27 \pm 1.28$ . Histopathological, analysis revealed reduced areas of muscular atrophy and hyalinization while morphometric analysis of gastrocnemius muscle inferred a significantly better healing in terms of muscle mass gain. Relative gene expression and scanning electron microscopic studies result revealed better, appreciable and organized sciatic nerve regeneration and optimum muscle mass gain post 90 days of scaffold treatment in groups E. This study helped us to understand that other than scaffold and stem cells, growth factors are also an important part in the regeneration of the nervous system.

## Acknowledgements

The authors wish to thank Prof. Partha Roy and Prof. Debrupa Lahiri, Biomaterial wing, IIT, Roorkee, India who scaffolded this study by generous supply of scaffold and also provided related literature. The authors also wish to thank the Director, ICAR-Indian Veterinary Research Institute, Izatnagar, India and Head, Division of Surgery, Indian Veterinary Research Institute for providing necessary facilities for this study.

### *Author contribution*

MM and SKM designed the study, analysed the data and prepared the manuscript; MM, KE, SS, AB, MM performed the experiments; DM helped in cell culture during COVID times; MA helped in biochemical estimation and SEM evaluation; KPS performed histopathological evaluation; JH edited the manuscript.

### *Funding*

There were no any external funding agencies supported to carry out this research. The research work was carried out in the ICAR-NAE project on "Development of stem cell laden nanomaterial scaffold for nerve, bone and cartilage tissue regeneration in animals".

### *Statement of Ethics*

Protocols for this study were approved by the Institutes Animal Ethical Committee for Animal Care and Animal Experimentation

## Disclosure Statement

All the authors confirmed that, there was no conflict of interest regarding publication of this manuscript.

## References

- 1 Navarro X, Vivo M, Valero-Cabre A: Neural plasticity after peripheral nerve injury and regeneration. *Prog Neurobiol* 2007;82:163-201.
- 2 Robinson LR: Traumatic injury to peripheral nerves. *Muscle Nerve* 2000;23:863-873.
- 3 Tajdaran K, Shoichet MS, Gordon T, Borschel GH: A novel polymeric drug delivery system for localized and sustained release of tacrolimus (FK506). *Biotechnology and Bioengineering* 2015;112:1948-1953.
- 4 Serpell CJ, Kostarelos K, Davis BG: Can carbon nanotubes deliver on their promise in biology? Harnessing unique properties for unparalleled applications. *ACS Cent Sci* 2016; 2:190-200.
- 5 Al Shehadat S, Gorduysus MO, Abdul-Hamid SS, Abdullah NA, Samsudin AR, Ahmad A: Optimization of scanning electron microscope technique for amniotic membrane investigation: A preliminary study. *Eur J Dent* 2018; 12:574-578.

- 6 Carriel V, Garrido-Gomez J, Hernandez-Cortes P, Garzon I, GarciaGarcia S, Saez-Moreno JA, Alaminos M: Combination of fibrin-agarose hydrogels and adipose-derived mesenchymal stem cells for peripheral nerve regeneration. *J Neural Eng* 2013; 10:14,
- 7 Chato-Astrain J, Campos F, Roda O, Miralles E, Durand-Herrera D, Saez-Moreno JA, Carriel V: In vivo evaluation of nanostructured fibrin-agarose hydrogels with mesenchymal stem cells for peripheral nerve repair. *Front Cell Neurosci* 2018; 1812:501-519.
- 8 Bain JR, Mackinnon SE, Hunter DA: .Functional evaluation of complete sciatic, peroneal and posterior tibial nerve lesions in the rat. *Plast Reconstr Surg* 1989;83:129-136.
- 9 Varejao AS, Cabrita AM, Geuna S, Melo-Pinto P, Filipe VM, Gramsbergen A Meek MF: Toe out angle: a functional index for the evaluation of sciatic nerve recovery in the rat model. *Exp Neurol* 2003; 183:695-699.
- 10 Tiwary R: Evaluation of nucleated marrow cells alongwith TGF- $\beta$ 1/IGF-1 for cartilage and nerve repair in rabbits. Thesis 2011, Ph.D. Deemed University, Indian Veterinary research Institute, Izatnagar, India. 224p.
- 11 Fraczek-Szczypta A: Carbon nanomaterials for nerve tissue stimulation and regeneration. *Mater Sci Eng C Mater Biol Appl* 2014; 34:35-49.
- 12 Taylor JSH, Bampton ETW: Factors secreted by schwann cells stimulate the regeneration of neonatal retinal ganglion cells. *J Anat* 2004; 204:25-31.
- 13 Algora J, Chen LE, Seaber AV, Wong GH, Urbaniak: Functional effects of lymphotoxin on crushed peripheral nerve. *Microsurgery* 1996; 17:131-135.
- 14 Rabinovsky ED, Gelir E, Gelir S: Targeted expression of IGF-1 transgene to skeletal muscle accelerates muscle and motor neuron regeneration. *FASEB Journal* 2003; 17:53-55.
- 15 Vergani L, Di Giulio AM, Losa M, Rossoni G, Muller EE, Gorio A: Systemic administration of insulin-like growth factor decreases motor neuron cell death and promotes muscle reinnervation. *J Neurosci Res* 1998; 54:840-847.
- 16 Rind HB, von Bartheld CS: Target-derived cardiotrophin-1 and insulin-like growth factor-I promote neurite growth and survival of developing oculomotor neurons. *Mol Cell Neurosci* 2002; 19:58-71.
- 17 Kaspar BK, Llado J, Sherkat N, Rothstein JD Gage FH: Retrograde viral delivery of IGF-1 prolongs survival in a mouse ALS model. *Science* 2003; 301:839-842.
- 18 Kanje M, Skottner A, Lundborg G Sjöberg J: Does insulin-like growth factor I (IGF-1) trigger the cell body reaction in the rat sciatic nerve? *Brain Res* 1991;563:285-287.
- 19 Svenningsen AF, Kanje: Insulin and the insulin-like growth factors I and II are mitogenic to cultured rat sciatic nerve segments and stimulate [3H] thymidine incorporation through their respective receptors. *Glia* 1996; 18:68-72.
- 20 Cheng HL, Russell JW, Feldman EL: IGF-I promotes peripheral nervous system myelination. *Ann N Y Acad Sci* 1999;883:124-130.
- 21 Sjöberg J, Kanje M: Insulin-like growth factor (IGF-1) as a stimulator of regeneration in the freeze-injured rat sciatic nerve. *Brain Res* 1989;485:102-108.
- 22 Lutz BS, Wei FC, Ma SF, Chuang DC: Effects of insulin-like growth factor I in motor nerve regeneration after nerve transection and repair vs. nerve crushing injury in the rat. *Acta Neurochirurgica (Wien)* 1999;141:1101-1106.
- 23 Tiangco DA, Papakonstantinou KC, Mullinax KA, Terzis JK: IGF-I and end-to-side nerve repair: a dose-response study. *Journal of Reconstructive Microsurgery* 2001;17:247-256.
- 24 Tamaddonfard E, Farshid AA, Ahmadian E, Hamidhoseyni A: Crocin enhanced functional recovery after sciatic nerve crush injury in rats. *Iran J Basic Med Sci* 2013;16:83-90.
- 25 Tan CW, Ng MH, Ohnmar H: Sciatic nerve repair with tissue engineered nerve: Olfactory ensheathing cells seeded poly(lactic-co-glycolic acid) conduit in an animal model. *IJOO* 2013;47:547-552,
- 26 Amniattalab A, Mohammadi R: Functional, Histopathological and Immunohistochemical Assessments of Cyclosporine A on Sciatic Nerve Regeneration Using Allografts: A Rat Sciatic Nerve Model. *Bull Emerg Traum* 2017;5:152-159 .
- 27 Farzamfar S, Salehi M, Tavangar SM: A novel polycaprolactone/carbon nanofiber composite as a conductive neural guidance channel: an in vitro and in vivo study. *Prog Biomater* 2019;8:239-248.
- 28 Khan AA, Faruqi NA, Ansari MS: Effects of hydrocortisone on the sciatic nerve crush injury in adult rat-a light microscopic study. *Curr Neurobiol* 2014;5:11-16.

- 29 Biazar E, Keshel SH, Pouya M: Behavioral evaluation of regenerated rat sciatic nerve by a nanofibrous PHBV conduit filled with Schwann cells as artificial nerve graft. *Cell Commun Adhes* 2013;20:93-103.
- 30 Johnson EO, Zoubos AB, Soucacos PN: Regeneration and repair of peripheral nerves. *Injury* 2005;36:24-29.
- 31 Raducan A, Mirica S, Duica O, Raducan S, Muntean D, Fira-Mladinescu O, Lighezan R: Morphological and functional aspects of sciatic nerve regeneration after crush injury. *Rom J Morphol Embryol* 2013;54:735.
- 32 Grasso G, Stacteria A, Brines M, Tomasello F: A new computed-assisted technique for experimental sciatic nerve analysis. *Med Sci Monit* 2004;10:BR1-BR3.
- 33 Monte-Raso Vilela V, Barbieri, Henrique C, Mazzer N: Sciatic functional index smashing injuries of rats' sciatic nerves. Evaluation of method reproducibility among examiners. *Acta Ortopédica Brasileira* 2006;14:133-136.
- 34 Gasparini ALP, Barbieri CH, Mazzer N: Correlation of different method of gait functional evaluation in rats with ischiatic nerve crushing injuries. *Acta Ortopédica Brasileira* 2001;15:285-289.
- 35 Baptista AF, de Souza Gomes JR, Oliviera JT, Santos SMG, Vannier-Santos MA, Martinez AMB: A new approach to assess function after sciatic nerve lesion in the mouse-adaptation of the sciatic nerve index. *J Neurosci Methods* 2007;161:259-264.
- 36 Kalaiselvan E: Stem cell laden nanomaterial – scaffold with or without growth factor for bone regeneration in rabbit. Thesis 2021, PhD. Indian Veterinary Research Institute, Izatnagar, Uttar Pradesh, India.
- 37 Higashino K, Matsuura T, Suganuma K, Yukata K, Nishisho T, Yasui N: Early changes in muscle atrophy and muscle fiber type conversion after spinal cord transection and peripheral nerve transection in rats. *J Neuroeng Rehabil* 2013;10:46.
- 38 El Gabbas Z, Bezza K, Laadraoui J, Ait Laaradia M, Kebbou A, Oufquir S, Boukhira A, Aboufatima R, Chait A. *Salvia officinalis*, Rosmarinic and Caffeic Acids Attenuate Neuropathic Pain and Improve Function Recovery after Sciatic Nerve Chronic Constriction in Mice. *Evid Based Complement Alternat Med*;2019:2370-2378.
- 39 Santiago LY, Clavijo-Alvarez J, Brayfield C, Rubin JP, Marra KG: Delivery of Adipose-Derived Precursor Cells for Peripheral Nerve Repair. *Cell Transplant* 2009;18:145-158.
- 40 Mimura T, Dezawa M, Kanno H, Sawada H, Yamamoto I: Peripheral nerve regeneration by transplantation of bone marrow stromal cell-derived Schwann cells in adult rats. *J Neurosurg* 2004;101:806-812.
- 41 Dadon-Nachum M, Sadan O, Sruago I: Differentiated Mesenchymal Stem Cells for Sciatic Nerve Injury. *Stem Cell Rev and Rep* 2011;7:664-671.
- 42 Cuevas P, Carceller F, Garcia-Gomez I, Yan M, Dujovny M: Bone marrow stromal cell implantation for peripheral nerve repair. *Neurol Res* 2004;26:230-232.
- 43 Chen X, Wang XD, Chen G, Lin WW, Yao J, Gu XS: Study of in vivo differentiation of rat bone marrow stromal cells into schwann cell like cells. *Microsurgery* 2006;26:111-115.
- 44 Shimizu S, Kitada M, Ishikawa H, Itokazu Y, Wakao S, Dezawa M: Peripheral nerve regeneration by in vitro differential human bone marrow stromal cells with Schwann cell property. *Biochem Biophys Res Commun* 2007;359:915-920.
- 45 Gneccchi M, Zhang Z, Ni A, Dzau VJ: Paracrine Mechanisms in Adult Stem Cell Signalling and Therapy. *Circ Res* 2008;103:1204-1219.
- 46 Caplan AI, Dennis JE: Mesenchymal stem cells as trophic mediators. *J Cell Biochem* 2006;98:1076-1084.
- 47 Prockop DJ: "Stemness" Does Not Explain the Repair of Many Tissues by Mesenchymal Stem/Multipotent Stromal Cells (MSCs). *Clin Pharmacol Ther* 2007;82:241-243.
- 48 Caplan AI: Adult mesenchymal cells for tissue engineering versus regenerative medicine. *J Cell Physiol* 2007;213:341-347.
- 49 Dubový P: Wallerian degeneration and peripheral nerve conditions for both axonal regeneration and neuropathic pain induction, *Annuals of Anatomy – Anatomischer Anzeiger* 2011;193:267-275.
- 50 Gu X, Ding F, Yang Y, Liu J: Construction of tissue engineered nerve grafts and their application in peripheral nerve regeneration. *Prog Neurobiol* 2011;93:204-230.
- 51 Goel RK, Suri V, Suri A, Sarkar C, Mohanty S, Sharma MC, Yadav PK, Srivastava A: Effect of bone marrow-derived mononuclear cells on nerve regeneration in the transection model of the rat sciatic nerve. *J Clin Neurosci* 2009;16:1211-1217.
- 52 Dezawa M, Takahashi I, Esaki M, Takano M, Sawada H: Sciatic nerve regeneration in rats induced by transplantation of in vitro differentiated bone marrow stromal cells. *Eur J Neurosci* 2001;14:1771-1776.

- 53 Shen LH, Li Y, Gao Q, Savant-Bhonsale S, Chopp M: Down-regulation of neurocan expression in reactive astrocytes promotes axonal regeneration and facilitates the neurorestorative effects of bone marrow stromal cells in the ischemic rat brain. *Glia* 2008;56:1747-1754.
- 54 Akiyama Y, Radtke C, Kocsis JD: Remyelination of rat spinal cord by transplantation of identified bone marrow stromal cells. *J Neurosci* 2002;22:6623-6630.
- 55 Nistor GI, Totoiu MO, Haque N, Carpenter MK, Keirstead HS: Human embryonic stem cells differentiate into oligodendrocytes in high purity and myelinate after spinal cord transplantation. *Glia* 2005;49:385-396.
- 56 Lindvall O, Kokaia Z: Stem cells for the treatment of neurological disorders. *Nature* 2006;441:1094-1096.
- 57 Lee H, Shamy AG, Elkabetz Y, Schofield CM, Harrision NL, Panagiotakos G, Socci ND, Tabar V, Studer L: Directed Differentiation and Transplantation of Human Embryonic Stem Cell-Derived Motoneurons. *Stem Cells* 2007; 25:1931-1939.
- 58 Munoz JR, Stoutenger BR, Robinson AP, Spees JL, Prockop DJ: Human stem progenitor cells from bone marrow promote neurogenesis of endogenous neural stemcells in the hippocampus of mice. *PNAS* 2005;102:18171-18176.
- 59 Liu CC, Zhao JJ, Zhang R: Multifunctionalization of graphene and graphene oxide for controlled release and targeted delivery of anticancer drugs. *Am J Transl Res* 2017;9:5197-5219.
- 60 Sivanarayanan TB: Evaluation of mesenchymal bone marrow derived mesenchymal stem cells with stem cell conditioned media for the repair of acute and subacute nerve injuries. Thesis 2015, PhD. Indian Veterinary Research Institute, Izatnagar, Uttar Pradesh, India.
- 61 Rore R, Piischel AW: The function of semaphorins during nervous system development. *Front Biosci* 2003;8:84-99.
- 62 Kitsukawa T, Shimizu M, Sanbo M, Hirata T, Taniguchi M, Bekku Yagi T, Fujisawa H: Neuropilin-Semaphorin III/D-Mediated Chemorepulsive Signals Play a Crucial Role in Peripheral Nerve Projection in Mice. *Neuron* 1997; 19:995-1005.
- 63 Kolodkin AL, Levensgood DV, Rowe EG, Tai YT, Giger RJ, Ginty DD: Neuropilin Is a Semaphorin III Receptor. *Cell* 1997;90:753-762.
- 64 Bagnard D, Thomasset N, Lohrum M, Puschei AW, Boiz J: Spatial distributions of guidance molecules regulate chemorepulsion and chemoattraction of growth cones. *J Neurosci* 2010;20:1030-1035.
- 65 Pasterkamp RJ, Anderson PN, Verhaagen J: Peripheral nerve injury fails to induce growth of lesioned ascending dorsal column axons into spinal cord scar tissue expressing the axon repellent Semaphorin-3A. *Eur J Neurosci* 2001;13:457-471.
- 66 Pasterkamp RJ, Winter FD, Giger RJ, Verhaagen J: Role for semaphorin III and its receptor neuropilin-1 in neuronal regeneration and scar formation? *Prog Brain Res* 1998;117:151-170.
- 67 Scariato M, Ara J, Bannerman P, Scherer S, Pleasure D: Induction of neuropillins-1 and -2 and their ligands, Sema3A, Sema3F, and VEGF, during Wallerian degeneration in the peripheral nervous system. *Exp Neurol* 2003;183:489-498.
- 68 Ara J, Bannermann P, Hahn A, Ramirez S, Pleasure D: Modulation of sciatic nerve expression of class 3 semaphorins by nerve injury. *Neurochem Res* 2004;29:1153-1159.
- 69 Hudson TW: Engineering of an optimized acellular peripheral nerve graft. Thesis 2003; PhD. University of Texas, Austin.